ENABLING REACTION WHEEL TECHNOLOGY FOR HIGH PERFORMANCE NANOSATELLITE ATTITUDE CONTROL

Doug Sinclair
Sinclair Interplanetary
268 Claremont Street, Toronto, Ontario, Canada, M6J 2N3
Tel: 647-286-3761; Fax: 775-860-5428; Web: www.sinclairinterplanetary.com
dns@sinclairinterplanetary.com

C. Cordell Grant, Robert E. Zee
Space Flight Laboratory
University of Toronto Institute for Aerospace Studies
4925 Dufferin Street, Toronto, Ontario, Canada, M3H 5T6
Tel: 416-667-7700; Fax: 416-667-7799; Web: www.utias-sfl.net
cgrant@utias-sfl.net, rzee@utias-sfl.net

ABSTRACT

To date nanosatellites have primarily relied on magnetic stabilization which is sufficient to meet thermal and communications needs but is not suited for most payloads. The ability to put one, or even three, reaction wheels on a spacecraft in the 2-20 kg range enables new classes of mission. With reaction wheels and an appropriate sensor suite a nanosatellite can point in arbitrary directions with accuracies on the order of a degree. Sinclair Interplanetary, in collaboration with the University of Toronto Space Flight Laboratory (SFL), has developed a reaction wheel suitable for very small spacecraft. It fits within a 5 x 5 x 4 cm box, weighs 185 g, and consumes only 100 mW of power at nominal speed. No pressurized enclosure is required, and the motor is custom made in one piece with the flywheel. The wheel is in mass production with sixteen flight units delivered, destined for the CanX series of nanosatellites. The first launch is expected in 2007. Future missions that will make use of these wheels include CanX-3 (BRITE), which will make astronomical observations that cannot be duplicated by any existing terrestrial facility, and CanX-4 and -5, which will demonstrate autonomous precision formation flying.

INTRODUCTION

Precise three-axis stabilization is a virtual necessity for any mission that requires a pointed instrument, whether the application is Earth observation, communications or astronomy. Until recently, the technology for precise pointing (a degree or less) has not been available for small missions. The Microvariability and Oscillations of STars space telescope was among the first to demonstrate arcsecond-level attitude stability on a 53-kilogram microsatellite platform. For microsatellites, the advent of precise three-axis attitude control has greatly expanded their utility. For nanosatellites, or satellites under 10 kilograms (or 20 kilograms, depending upon the naming convention used), the enabling technology for precise three-axis attitude control has so far been nascent. One key enabling technology is the reaction wheel. Although various organizations have attempted to create reaction wheels for nanosatellites, subject to the physical and financial constraints of typical nanosatellite programs, there are currently no products on the market that fill this need.

In recognition of this need, and in order to meet the stringent requirements of missions under development at the University of Toronto's Space Flight Laboratory (SFL), Sinclair Interplanetary has developed a low-cost, scalable/customizable reaction wheel for nanosatellites in collaboration with SFL. At present, sixteen wheels have been produced to support three nanosatellite missions under development at SFL: CanX-2 (Canadian Advanced Nanospace eXperiment 2), BRIght Target Explorer (BRITE) Constellation (aka CanX-3), and CanX-4/CanX-5 formation flying. CanX-2, a 3.5 kg, 10x10x34cm satellite launching from India in 2007 aboard the Polar Satellite Launch Vehicle, is carrying a reaction wheel prototype for testing in space. BRITE Constellation and the CanX-4&5 formation flying mission involve multiple 20cm cube satellites, each equipped with three reaction wheels for precise pointing. BRITE Constellation is a space astronomy mission that requires 1.5 arcminute pointing stability, while CanX-4 and CanX-5 require relatively fast slews (90º in 60 seconds) to point thrusters for orbital maintenance. Neither mission

would be possible without nanosatellite reaction wheels.

This paper describes the innovative design of the Sinclair-SFL nanosatellite reaction wheel (Figure 1). Its advantages include scalability and low-cost by virtue of a custom motor design that does not require a pressurized container. The Sinclair-SFL wheel is available as a Canadian technology for use by any future nanosatellite program that requires precise one-, two- or three-axis attitude control.

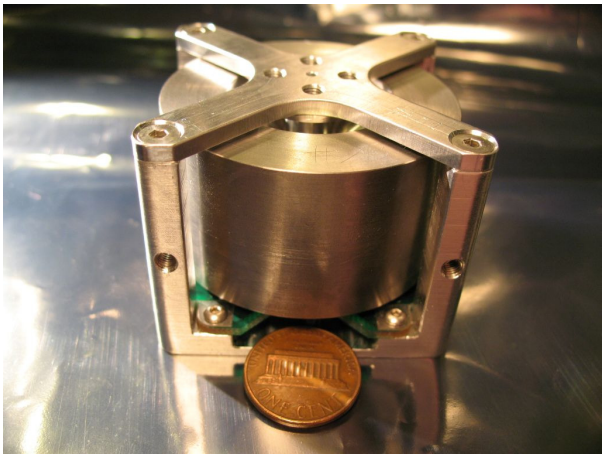

Figure 1: Reaction Wheel with Penny for Scale

SPECIFICATIONS

Table 1: Wheel Specifications

Mass	185 g
Dimensions	5 x 5 x 4 cm
Power, Max Speed	0.4 W @ 30 mNm-sec
Power, Nominal	0.1 W @ 10 mNm-sec
Max torque	2 mNm
Supply Voltage	+3.3 V to +6.0 V
Command and Telemetry	Asynch serial 19.2 kbps
Connector	4-pin DF11
Temperature, Operational	-35ºC to +60ºC
Temperature, Survival	-40ºC to +100ºC

Table 1 shows the specifications for the wheels delivered to the CanX satellites. The design concept is easily expandable. Work is ongoing on a mechanical upgrade to a 6.5 x 6.5 x 4 cm package capable of 60 mNm-sec. An electronics upgrade is also considered that would allow +12 V input power and a more robust MIL-C-83513 micro-D connector. The command and telemetry interface may be freely changed from asynchronous serial to SPI, I2C or CAN.

COMMERCIAL MOTORS

Tiny electric motors are commercially available for a host of applications: toys, pagers, dental equipment and the like. Upon cursory inspection some of these might seem to be useful for a small reaction wheel. Detailed investigation, however, shows that none are ideal. To get the motor that we really wanted for this project we had to build it ourselves.

Several classes of COTS motors can be immediately discarded. DC brush motors do not have the lifetime for multi-year space missions; the brushes simply wear down after thousands of hours of continuous rotation. Motors that do not contain permanent magnets (e.g. steppers, AC motors, switched-reluctance motors) have unacceptably high hysteresis power losses.

Brushless DC motors are most suitable for reaction wheels, and a number of micro- and nano-satellite projects have used commercial motors at the hearts of their wheels. Even so, these parts suffer from a number of restrictions.

Small commercial brushless motors typically use a two-pole magnetic design. Leakage flux from a stationary motor causes a parasitic dipole moment on the spacecraft that may produce unwanted attitude torques. The small number of poles means that there are only six commutation events per revolution and so speed measurement becomes difficult at low speed without additional encoders.

The motors contain two internal ball bearings with a light axial preload. Off-the-shelf parts use standard grease that is unsuitable for space. Motors with vacuum-greased bearings may sometimes be special-ordered from the factory but at increased cost and lead-time. Even with the correct lubricant the bearings, preload, and shaft-diameter are typically undersized for vibration loads. A naïve design that simply presses a wheel onto the end of the motor shaft is unlikely to survive launch.

Redundancy is essentially unknown in the commercial world. Motors with isolated windings or auxiliary sensors simply cannot be bought. For many nanosatellite programs this is acceptable, but it makes it impossible to migrate the design towards high-reliability.

The majority of commercial brushless motors are designed for servo applications. Much design effort has gone into minimizing their inertias so that they can achieve rapid accelerations. To take such a motor and couple it to a high inertia flywheel defeats the purpose and results in a non-optimal design.

CUSTOM MOTOR CONCEPT

Realizing that mating a low-inertia motor to a high-inertia wheel makes no sense we attempted a different tack. What if we could design a brushless DC motor that was optimized for high inertia? If the inertia of the motor itself is large enough then there is no need for a separate wheel. The two concepts join into a single rotor element.

The first step in the concept evolution is to turn the traditional brushless motor configuration inside out. The heavy magnets are now at a large radius from the center so they contribute usefully to the inertia. The windings are now on the outside of a cylindrical stator instead of on the inside, making fabrication much easier.

The second step is to spin the back-iron. The back-iron on the outside of a conventional motor prevents field-lines from leaving, increasing torque and suppressing radiated emissions. It is normally subjected to rotating magnetization, and thus must be made from ferrite or laminated steel to prevent eddy-current losses. If the back-iron is spun, however, it sees only DC magnetization! There are no eddy-current or hysteresis losses and it can be made from solid steel. A rotating back-iron both increases the inertia and reduces the motor's magnetic losses.

The large inner circumference of the rotor allows many poles to be comfortably spaced. More poles reduce radiated magnetic fields, give more commutation events from which speed can be determined, and push torque-ripple up to higher frequencies. A sketch of the motor concept is shown in Figure 2. For clarity a four-pole motor is shown; flight-models use a ten-pole motor.

The red lines illustrate the magnetic field loops. Each magnetic circuit travels approximately half its distance in the rotor back-iron and half through the non-magnetic stator and air-gap. The path reluctance is high, and so large magnets are required to achieve high field strength. As the magnets contribute usefully to the rotor inertia this is not a particular problem.

Three-phase windings require three coils for each pole-pair. The motor illustrated here has six coils for a four-pole rotor. The flight motor have fifteen coils to go with the ten-pole rotor. The coils are wound in slots on a Delrin stator. Unlike the slots in a traditional steel stator these slots serve no magnetic function – they simply provide mechanical support for the wire.

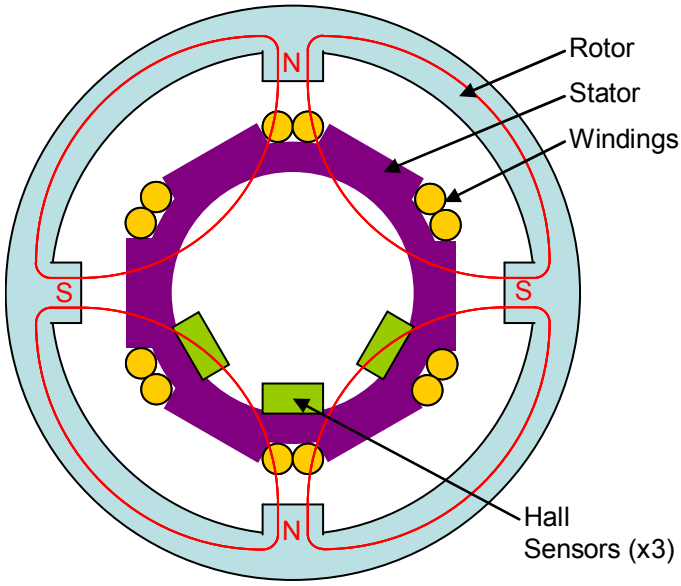

Figure 2: Magnetic Schematic of Motor

Three digital Hall-effect sensors are mounted to the stator behind the windings. They detect the passage of the rotor magnets and are used for both commutation and for speed measurement.

MAGNETIC DESIGN

Once the concept was developed there were quantitative design considerations. How many poles should there be? How much clearance should there be between rotor and stator? How many turns of wire are needed, and of what gauge?

Precise analytical modeling is very difficult. The problem is three-dimensional and the B-H curves of the magnets are non-linear. Sophisticated finite-element tools are available that might be used, but we took a much simpler approach to the engineering.

For the first pass, a paper-and-pencil analysis of the magnetic fields was performed. The field shapes were sketched heuristically, and the resulting geometry used to determine the strengths. This gave us confidence that the design was feasible, and in the end proved to be remarkably accurate.

The second pass was performed empirically. It turns out that a small metalworking lathe is an invaluable tool for prototyping reaction wheels. It can obviously be used to make test parts. Once that is done, however, it can be used experimentally. A test rotor complete with magnets is chucked into the lathe and spun. A small wire coil of known dimensions is attached to a wooden stick which is clamped into the lathe's tool holder. An oscilloscope measures the back-EMF, from which dB/dt can be calculated. The coil can be precisely

translated using the lathe's handwheels, and so the field at different points inside the rotor can be mapped.

Figure 3: Lathe as Test Instrument

In this special case we feel that experimentation was faster and cheaper than computer modeling, with added confidence that the data reflects reality.

WINDINGS

An ideal brushless DC motor should exhibit an equal sinusoidal back-EMF voltage waveform in each phase. This motor is far from ideal. The discrete spacing of the poles and the windings leads to third-order harmonics. The manual winding process leads to certain phases having higher back-EMF amplitudes than others. Building a high-performance wheel requires accounting for these non-idealities.

A consequence of the poor phase-to-phase voltage match is that a Δ-winding configuration is impossible. Δ-winding requires that the sum of the three winding voltages is always zero. When it is not, circulating currents develop in the coils which contribute a drag torque. Instead this motor is Y-wound. It eliminates circulating currents at the cost of slightly less efficient copper usage.

Each phase is composed of two conductors wound bifilar and connected in parallel at the end points. This provides redundancy in the event of wire breakage. By using two smaller wires instead of one of a heavier gauge the eddy currents in the copper are reduced and thus the drag torque is decreased.

SOFTWARE

The reaction wheel incorporates a mixed-signal microcontroller as central part of its electronics. This replaces many of the analog functions in a traditional wheel and leads to a radical decrease in parts count.

Figure 4 shows a block diagram of the software in the microcontroller when configured as a closed-loop speed servo. There are two nested feedback systems: a high-rate power-control loop and a low-rate speed-control loop.

The power-control loop occupies the top-right quadrant of the figure. The microprocessor's ADC is used to sample the instantaneous current and voltage in the motor. These readings are multiplied, subtracted from the power setpoint, and fed into a saturating integral controller. The output goes into a DAC that drives the motor's analog pulse-width modulator circuits.

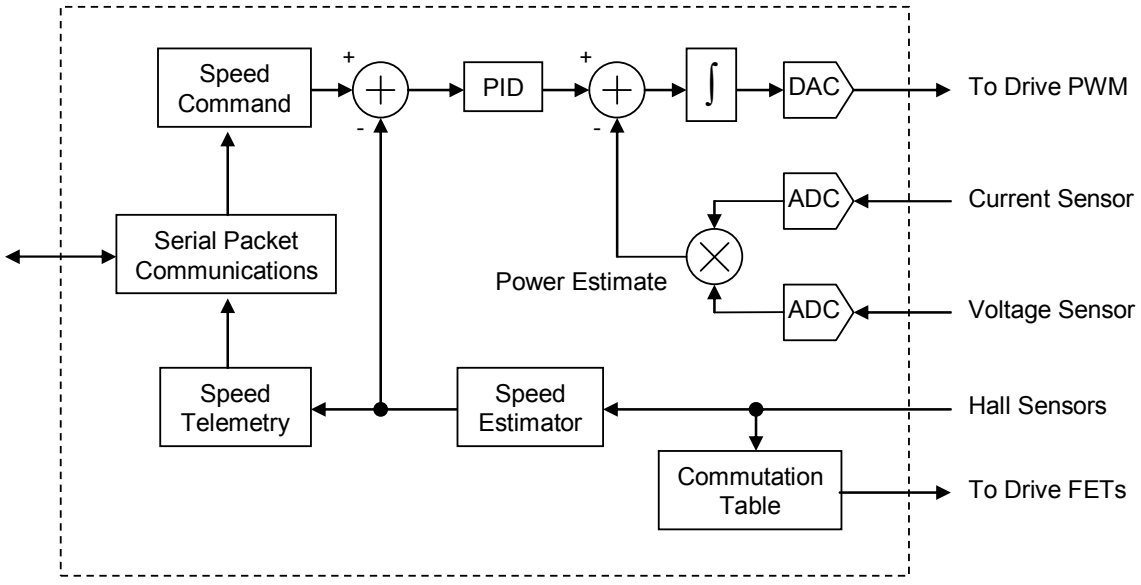

Figure 4: Speed-Mode Software Block Diagram

This software block executes at a rate of 55 kHz, phase-locked to the 440 kHz switching PWM. By controlling the motor power, instead of the more common current or voltage, low torque ripple is maintained even with non-ideal winding back-EMF waveforms. The algorithm uses only fixed-point arithmetic and is hand-coded in assembly language to achieve the required speed.

The speed-control loop runs at a more leisurely 93 Hz and is coded in C with floating-point arithmetic. Hardware capture peripherals detect the transition-times of the Hall sensors to a resolution of 200 nsec. By measuring the time taken for a complete 360º wheel rotation the instantaneous speed can be precisely estimated. In particular, measurement over a full circle cancels any errors due to magnet irregularities or Hall sensor placement. The wheel speed is subtracted from the speed setpoint and fed into a PID controller. The output of this controller is used as the setpoint input of the power-control loop.

On the left of the figure is the communications block. All commands and telemetry flow through the packet communications logic. A wide variety of telemetry is available in addition to speed: voltage, current, temperature, and a host of software status values. Similarly, commands may be used to adjust controller gains and saturation limits. Other operating modes are also available. Some spacecraft may prefer to operate in closed-loop torque mode, while open-loop modes were used during development.

The operating software for the wheel is stored in on-chip Flash memory. The packet communications driver can be used to upload new programs that can be run on command. This allows software to be patched on-orbit if need be. The communications code itself cannot be modified, and the spacecraft can return the wheel to a known-good state at any time by a power cycle. If erroneous software is accidentally loaded it can be erased and rewritten without risk.

A final feature of the wheel software is the built-in test mode. The wheel can be commanded to execute a standard test sequence with a duration of several minutes. The test measures a number of critical variables: speed tracking error, bearing friction, and winding resistance of each phase. The sequence is used during manufacture after assembly, and then again after vibration and thermal cycles. It can be run at the spacecraft level after integration, and again after TVAC. It can even be run on-orbit. The single test sequence makes it easy to immediately compare before and after data to detect changes in wheel performance. Such automation is fiscally necessary when building a large number of parts for low-cost missions.

STRUCTURE

The wheel is held in an open box-shaped frame which supports the bearings, electronics and motor. The trade-off between a closed container and an open frame is interesting.

Many small satellite wheels use a hermetic housing filled with a low-pressure gas. The internal atmosphere allows the use of bearing lubricants with modest vapour pressures as well as protecting parts from contamination or damage.

By forgoing the enclosure we have been forced to use vacuum-compatible lubricant in the bearings. These greases tend to be quite thick, and they increase the friction losses at a given speed. However the lack of a container means that the wheel diameter can be increased and still remain within the target footprint. Increased diameter leads to greatly increased inertia, which in turn means that the wheel can operate at lower speed for a given angular momentum. Comparing a high-speed bearing with regular lubricant to a low-speed bearing with vacuum lubricant the frictional losses are similar.

There are many advantages to an open-frame wheel. The structure mass drops radically. We need no fill valves, or other fittings to pump out air during integration. There is no seal-leak failure mode, and no need for an internal pressure telemetry point. There is no windage loss on-orbit (though there is considerable aerodynamic loss in the lab).

Most wheels only have mounting points on the bottom plate, making it difficult to arrange three orthogonal units without extensive brackets. By replacing the container with an open frame we have added threaded hardpoints on three additional faces giving much more mounting flexibility.

The obvious down-side to an open concept wheel is its vulnerability to external disturbance. This design is robust against moderate chemical and dust contamination. It uses no optical encoders, passivates all metal surfaces, and uses shielded bearings with fluorinated lubricant. The most serious threat is that a large object in the spacecraft could get loose and press against the rotor. Wire bundles in particular must be carefully routed and restrained to prevent them from coming into contact.

CONCLUSION

A number of groups, several involving the author, have previously attempted to bring nanosatellite wheels to market. They have produced limited quantities of flight hardware but for various reasons the wheels have not been commercially successful and have not been available to small satellite designers. Now, with sixteen delivered and interest from several other parties, Sinclair Interplanetary and SFL believe that they have succeeded. A wheel is now available to nanosatellite builders at a price that is consistent with low-cost research missions.

The key to our success has been to design the wheel from the ground-up for simplicity. It does not use a commercial motor, or any bought-in subassembly more complex than a bearing or a computer chip. This ensures complete control of the materials and processes and eliminates the chain of specialized suppliers that might otherwise drive the cost and the lead-time. Experience shows that the labour to build such a unit is no greater than that required to assemble a traditional wheel from more complex integrated parts.

In the past ten years we have seen a host of new missions opened up for microsatellites with the advent of reaction wheels in the ~1 kg class. Space astronomy, earth observation and narrow-spot communication payloads which were traditionally reserved for very large busses are now feasible for spacecraft in the 30 – 100 kg range. We have now introduced a wheel in the 0.2 kg class, and expect it to enable similar missions for spacecraft in the 2 – 20 kg range. Already SFL is using it for astronomy and formation-flying maneuvers. We look forward to the missions that others may find for it.

ACKNOWLEDGEMENTS

The authors gratefully acknowledge the support of the Ontario Centres of Excellence Inc. (ETech Division) and the Canadian Space Agency.